Deep–Sea Research I 198 (2023) 104076

Contents lists available at ScienceDirect

Deep-Sea Research Part I

journal homepage: www.elsevier.com/locate/dsri

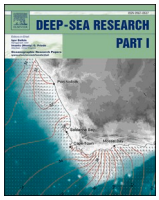

Spatiotemporal variability of micronekton at two central North Pacific Fronts

Réka Domokos

Pacific Islands Fisheries Science Center, NMFS, NOAA, 1845 Wasp Boulevard, Bldg. 176, Honolulu, HI, 96818, USA

ARTICLE INFO

Keywords:
North Pacific subtropical frontal zone (STFZ)
Subtropical front (STF)
Transition zone chlorophyll front (TZCF)
Micronekton
Acoustic scattering layers
Environmental forcing

ABSTRACT

The North Pacific Subtropical Frontal Zone (STFZ) seasonally aggregates economically important fish and protected species. The aggregation of top predators is hypothesized to be a response to convergent flow at the prominent thermohaline Subtropical Front (STF) in the STFZ and a sharp northward increase in primary productivity, the Transition Zone Chlorophyll Front (TZCF), which is thought to link primary productivity to top predators via secondary and tertiary consumers. Given existing data gaps in our knowledge on forage biomass, distribution, and composition in the area, characteristics of micronekton, forage for top predators, were investigated using *in situ* multi-frequency active acoustics from three springtime shipboard surveys conducted along the 158°W meridional. The effects of STF and TZCF on micronekton was accessed using *in situ* CTD profiles. Results of this study showed a significant positive effect of the STF on micronekton biomass. The acoustic data implied that the STF also acted as a boundary for the distribution of micronekton with differing taxonomic composition from south to its north. The TZCF, as well as Chl-a concentrations, did not show a significant effect on micronekton relative biomass or composition that might be due to effects of larger-scale variability masked in the *in situ* data. Contrary to expectation, significantly higher relative micronekton biomass was associated with higher temperatures, the mechanisms of which still need to be determined.

1. Introduction

Oceanic convergent frontal regions are known to aggregate marine fauna across the trophic spectrum, including economically-important and protected species. One such basin-scale convergent region is the North Pacific Transition Zone where the cool, low-salinity, productive waters from the subarctic gyre sink below the warm, saline, oligotrophic subtropical gyre waters of the North Pacific Ocean (Fig. 1). In the central Pacific, this convergent region serves as a "nutrition highway" for several pelagic predator species, such as elephant seals (e.g., Block et al., 2011; Hazen et al., 2013; Polovina et al., 2017; Robinson et al., 2012), marine birds (Hyrenbach et al., 2002), loggerhead turtles (Polovina et al., 2004; 2000), and swordfish (Seki et al., 2002). The importance of the dynamic North Pacific Transition Zone to top predators has been recognized by the commercial fishing industry, and the zone is an important fishing ground for international fleets targeting species such as Pacific pomfret, albacore, and swordfish (Polovina et al., 2001; Seki et al., 2002). These species are hypothesized to be attracted to the region by the availability of highly nutritious prey (e.g., Pearcy, 1991). The success of the Hawaii-based longline fishery that targets bigeye and yellowfin tuna (WPRFMC, 2017) and swordfish (Seki et al., 2002) in the central and eastern Pacific is affected by the seasonally and interannually varying Subtropical Frontal Zone (STFZ) that forms the southern boundary of the North Pacific Frontal Zone. Its latitudinal position also influences survival of endangered Hawaiian monk seals and their pups in the Northwestern Hawaiian Islands, presumably by affecting the abundance of prey (Baker et al., 2007; Parrish et al., 2012), as well as increases bycatch of juvenile loggerhead turtles (Howell et al., 2008) when turtles occupy regions coinciding with those of the targeted swordfish.

The STFZ is composed of several fronts that have been defined by different properties. One of the most prominent fronts is a strong, meandering thermohaline front (Roden, 1991; Shcherbina et al., 2009, 2010), the Subtropical Front (STF – see Fig. 2, top panels). The STF is characterized by relatively strong mesoscale eddy activity and enhanced vertical mixing and defined as the surface expression of the 34.8 isohaline and the 17–18 °C isotherm that moves from 40° to 45°N during July–September to 30°-35°N during January–March (Polovina et al., 2001; Roden, 1991; Seki et al., 2002). The STFZ is also characterized by a sharp increase (from south to north) in surface chlorophyll

E-mail address: reka.domokos@noaa.gov.

https://doi.org/10.1016/j.dsr.2023.104076
Received 11 February 2023; Received in revised form 19 May 2023; Accepted 29 May 2023
Available online 30 May 2023

concentrations, and this steep gradient defines the Transition Zone Chlorophyll Front (TZCF – see Fig. 2, bottom panels). The TZCF is marked by the surface expression of 0.20 mg m^{-3} chlorophyll concentrations.

The latitudinal position of the STF is governed by atmospheric pressure and wind stress forcing on the rotating earth, resulting in current velocity shear, thermohaline stratification, and heat and salinity fluxes (Roden, 1991; Shcherbina et al., 2009, 2010), while the governing forces for the position of the TZCF are less clearly understood. High productivity associated with the TZCF is thought to be driven by vertical mixing due to the meandering STF (Seki et al., 2004; Wilson et al., 2013), but other reports suggest that it is driven by Ekman flow (Ayers and Lozier, 2010; Bograd et al., 2004; Howell et al., 2017; Juranek et al., 2012). The high productivity and chlorophyll blooms in the region can support the aggregation of higher trophic level organisms (e.g., microzooplankton and micronekton like krill and small mesopelagic fishes and squids) that can serve as an area of rich forage for a wide variety of marine predators (Seki et al., 2004). Historically, the latitudinal positions of the STF and TZCF are coincident in space west of 155°W, but to the east, the TZCF bifurcates north of the STF due to due to characteristic large-scale patterns in the prevailing winds (Bograd et al., 2004; Polovina et al., 2001).

In the early 2000s, concerns over bycatch, as well as efforts to transition toward implementation of Ecosystem-Based Fisheries Management, spurred a comprehensive effort to understand the dynamics and the effects of the STFZ on targeted and protected species (Polovina et al., 2017). Based on the assumption that top predators aggregate at the STFZ via bottom-up forcing, most of this research focused on the TZCF, although its latitudinal position often approximated by the 18 °C sea-surface temperature (SST) (Howell et al., 2008, 2015). But approximating the position of TZCF via SST prevents assessment of the distinct roles of the physical and biological fronts might have on top predators and their forage micronekton. Despite the known influences of forage distribution and abundance on the movement and distribution of their predators (e.g., Domokos, 2009; Green et al., 2020; Josse et al., 1998; Lambert et al., 2014; Menkes et al., 2015; Miller et al., 2018; Pérez-Jorge et al., 2020), our knowledge of the effects of STFZ on micronekton (Brodeur et al., 2005), is very limited. Besides the availability of secondary trophic level organisms as prey, temperature and oxygen are known to affect the distribution, composition, and abundance of micronekton (Domokos et al., 2007; Escobar-Flores et al., 2013; Fennell and Rose, 2015; Hazen and Johnston, 2010; Receveur et al., 2020a, 2020b).

To help increase our understanding and ability to predict abundance and distribution of high trophic-level organisms, knowledge of the distribution, composition, and biomass of micronekton is essential (e.g., Kloser et al., 2009; Menkes et al., 2015). However, information on North Pacific micronekton are limited to regions more readily accessible by ships equipped with active acoustics and/or trawling equipment that are typically used to survey micronekton. Active acoustics can provide spatiotemporally continuous data over large spatiotemporal regions but interpretation of acoustics signals are limited without a priori knowledge of type and size-range of the ensonified organisms (Benoit-Bird and Lawson, 2016; Simmonds and MacLennan, 2005). On the contrary, net samples can provide specific species and size information but sampling is limited spatiotemporally (Merrett et al., 1991) and can be biased due to their spatiotemporal limitations, selectivity of the net, and avoidance (De Robertis et al., 2017; Kaartvedt et al., 2012; McClatchie et al., 2000; Song et al., 2022) Combination of these methods, complemented by optical observation can provide more accurate micronekton biomass estimates than either of these methods alone (Benoit-Bird et al., 2008; Doray et al., 2007; Escobar-Flores et al., 2022; McClatchie et al., 2000). However, given the remoteness of the STFZ in the central Pacific, current information is limited to a few acoustic surveys, net sampling, and video observations from regions adjacent to continents or other large land masses, such as off Japan, the Kuroshio Current region, the Bering Sea, south of the Aleutian Islands, the California Current region, and the Hawaii Archipelago (summarized by Brodeur and Yamamura, 2005; and Song et al., 2022), or stomach content analyses of lesser known predatory fish in the central North Pacific (Choy et al., 2016).

The objectives of this study were to confirm or reject the hypotheses that 1) enhanced micronekton biomass is associated with the STFZ, 2) the composition of micronekton is different from the south of the STFZ to its north, 3) increased chlorophyll concentrations (and the TZCF) are responsible for any observed effects. In addition to finding answers to these questions, the observed characteristics of the STFZ are examined considering its expected sensitivity of the region to larger-scale variability and change.

2. Data and methods

To examine the effects of STF and TZCF on micronekton, *in situ* data (available at Pacific Islands Fisheries Science Center, 2015; Pacific Islands Fisheries Science Center, 2011; Pacific Islands Fisheries Science Center, 2009) were collected on board the NOAA Ship *Oscar Elton Sette* along three meridional surveys from the subtropical gyre, north of Oahu,

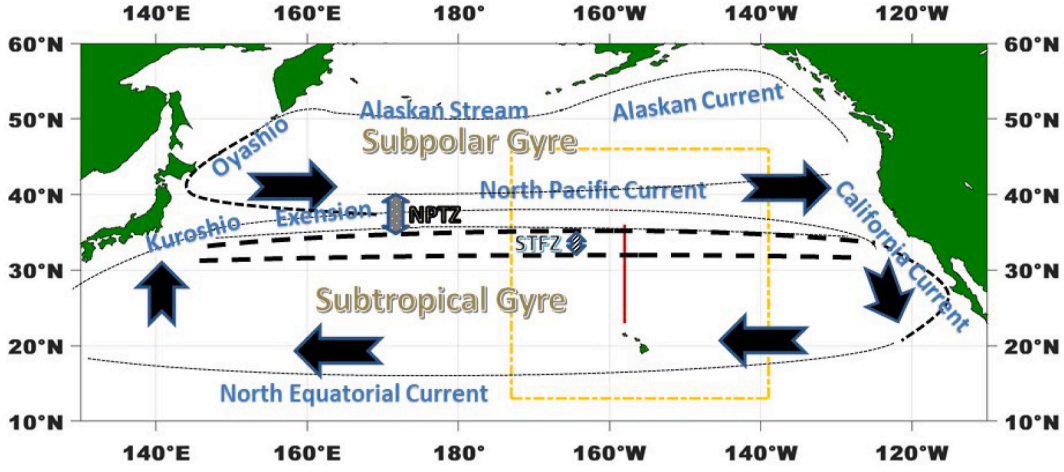

Fig. 1. Schematic representation of the major current systems of the North Pacific Ocean. The vertical line along the 158°W meridian represents the nominal survey location, with the box bounded by dash-dotted lines denoting the area represented in Fig. 2. The North Pacific Transition Zone is located between the Subpolar and Subtropical Gyres bounded by the Subtropical Frontal Zone (STFZ) to the south. The STFZ is the location of the Subtropical Front (STF) and the Transition Zone Chlorophyll Front (TZCF).

Hawaii, to the STFZ. The surveys were conducted along the 158°W meridian during spring of 2009 (22.5–36.0°N, March 17–22), 2011 (23–36.0°N, March 10–25), and 2015 (22.5–32.5°N, April 4–14) in the central North Pacific (Fig. 1). Small deviations from the 158°W meridian were necessary during the 2011 northbound transect due to heavy weather north of 32°N and in 2015 due to time limitations to reach the TZCF that extended further south to the west of 158°W based on concurrent satellite maps (Fig. 2).

2.1. Oceanographic characteristics

In situ hydrographic data were collected down to 1000 m depth at stations along the transects using a SBE 9⁄11+ CTD system equipped with redundant temperature, conductivity, and dissolved oxygen sensors and a Seapoint fluorometer for in vivo chloropigment (chlorophyll + phaeopigments) determinations. Hydrographic stations were conducted every 0.25° during the northbound transect in 2009 (55 stations), during the northbound and southbound transects in 2011 (37 and 41 stations), and during the southbound transect in 2015 (25 stations). Fluorometer data from a Turner Designs model 10-AU fluorometer were corrected and chlorophyll-a (Chl-a) extracted using liquid chromatography on *in-situ* water samples, as described by Howell et al. (2017). To assess the positions of the STF (P_{STF}) and the TZCF (P_{TZCF}), the upper mean 20-m water-column averages of the discrete CTD-derived salinity and chlorophyll-a values were used. The positions of the fronts were defined where the upper 20-m mean salinity values reached ≤34.8 PSU for the P_{STF} and the three consecutive mean upper 20-m chlorophyll concentrations reached ≥0.2 mg m^{-3} for the P_{TZCF}, respectively, a method adapted from Howell et al. (2017). Meridional averaging of the Chl-a values were necessary to avoid non-contiguous patches in the *in-situ* data (Howell et al., 2017). The P_{STF} obtained from the salinity data corresponded to the positions of the upper 20-m mean temperature values reaching ≤17.7 °C, within the expected range of the signature of the STF.

2.2. Micronekton distribution

1. Acoustic surveys

Micronekton horizontal and vertical distribution, relative biomass, and density were estimated using active acoustic methods. *In situ* acoustic backscatter data were collected aboard the NOAA Ship *Oscar Elton Sette* continuously during the 2009, 2011, and 2015 surveys at 38, 70, and 120 kHz frequencies. The *Sette* is equipped with a hull-mounted split-beam (7° circular angle), narrow-band Simrad EK60 system that was calibrated prior to each survey using a 38.1-mm-diameter tungsten carbide sphere and standard methods (Demer et al., 2015). The system was set to operate with 1024 μs pulse lengths at 2.00, 0.75, and 0.25 kW power for the 38, 70, and 120 kHz channels, respectively. Mean volume backscattering strengths (MVBS, in dB re 1 m^{-1}), were thresholded to −75 dB to avoid backscatter from plankton and other smaller organisms. These settings gave approximate ranges of 1600, 750, and 300 m at 38, 70, and 120 kHz, respectively, with a 10-dB minimum signal-to-noise ratio (SNR) at maximum depths. Data were recorded down to 1200-m

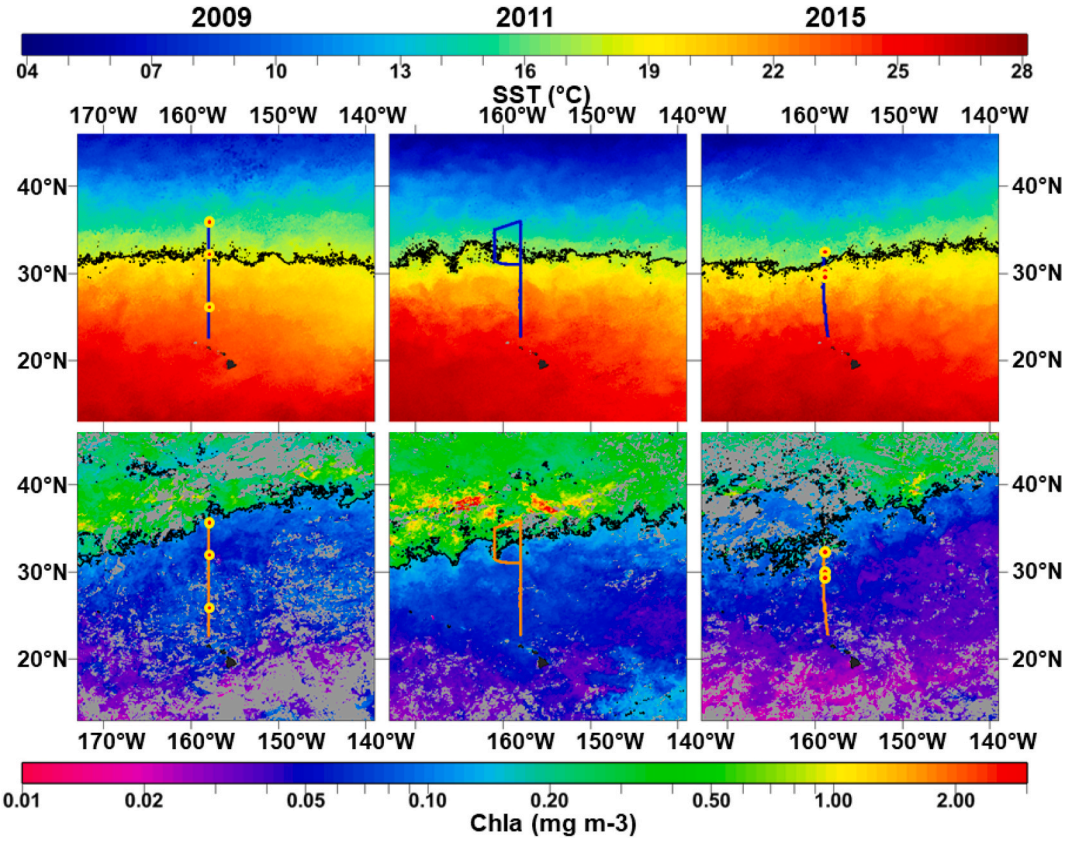

Fig. 2. Monthly SST (Pathfinder AVHRR v4.1, http://oceanwatch.pifsc.noaa.gov/erddap/griddap/OceanWatch_pfgac_sst_monthly.graph) and surface Chl-a (MODIS Aqua http://oceanwatch.pifsc.noaa.gov/erddap/griddap/OceanWatch_aqua_Chl-a_monthly.graph) over an area of the central North Pacific for months corresponding to the Surveys (March for 2009 and 2011, April for 2015). Black contours indicate the position of the Subtropical Front (surface expression of the 17.7 °C contour) and the Transition Zone Chlorophyll Front (surface expression of the 0.2 mg m^{-3} contour) on the SST and Chl-a maps, respectively. Shipboard survey transects are indicated by dark blue (SST) and orange (Chl-a) lines for the (from left) 2009, 2011, and 2015 Surveys. Red circles with yellow edges indicate the positions of the 2009 and 2015 trawl stations. Note the main Hawaiian Islands are shown in dark gray at the southern tip of transects. Missing data due to cloud cover are indicated in light gray on the Chl-a maps.

depth with the upper 15 m discarded to avoid near-field (nonlinear) effects and intermittent bubble noise due to inclement weather.

Prior to processing the acoustic data, pings impacted by cavitation noise and bubble dropout were removed using Echoview software (Echoview Software Pty Ltd, Hobart, Tasmania) then visually scrutinized to ensure high quality of the data. Based on semivariograms, the elementary data sampling unit (EDSU) was defined as 1-nmi long and 10-m deep. MVBS were averaged per EDSUs and vertically integrated to obtain nautical area scattering coefficients (NASC in m^2 nmi^{-2}) to be used for analyses. MVBS and NASC values are proportional to the density and biomass of organisms, respectively, when their composition is relatively stable, since organisms' backscatter characteristics depend on their physiology, morphology, size, orientation, and frequency (Lawson et al., 2008; Simmonds and MacLennan, 2005). For example, while the use of 38 kHz backscatter as proxy for relative biomass is well established in the literature (e.g., Cascão et al., 2019; Irigoien et al., 2014; Kloser et al., 2009; Proud et al., 2015), it can provide biased estimates as that frequency is dominated by micronektonic fish and/or gelatinous organisms with gas inclusions (e.g., Dornan et al., 2019). In scattering layers of heterogeneous composition, multi-frequency acoustics enable the classification of organisms into key groups based on their distinct frequency-dependent responses (de Robertis et al., 2010; Jech and Michaels, 2006; Korneliussen et al., 2008) and allow for the interpretation the acoustic signals in scattering layers of diverse composition (e.g., Béhagle et al., 2017; Benoit-Bird and Lawson, 2016; Fernandes, 2005; Korneliussen et al., 2008; Simmonds and MacLennan, 2005). Given the expectations of significant changes in micronekton composition across large zonal fronts, the use of NASC from all frequencies were necessary to provide relative biomass and basic composition estimates.

Since micronekton form ubiquitous dense shallow and deep scattering layers (SSL and DSL) (e.g., Benoit-Bird et al., 2016; Proud et al., 2017, 2015) and many undergo diel vertical migration (DVM) between the SSL and DSL or below (D'Elia et al., 2016; Solberg and Kaartvedt, 2017), the density and the vertical position and extent of the layers exhibit pronounced diel differences. Therefore, backscatter from the SSL and DSL from daytime and nighttime were assessed separately. Based on visual inspection of the echograms, vertical integrals of NASC from above and below 300-m were assigned to the SSL and DSL, respectively, and "water-column" (WC) data refer to integrals from the surface to the depth of recording. Based on echograms, excluding data from 05:00–08:00 and 17:00–20:00 were deemed sufficient to omit crepuscular periods, during which organisms underwent DVM.

2. Trawl sampling

To aid the interpretation of the acoustic data, simultaneous acoustic and trawling operations were conducted at predetermined latitudes using a midwater Cobb trawl with a ~140 m^2 mouth opening and mesh size decreasing from 152 mm at the mouth to a cod-end of 3.2 mm (described in detail by Drazen et al., 2011). However, due to the failure of the *Sette*'s trawling system and time limitations, the number of successful trawls were limited to tows at 26°N, 32°N, and 36°N during the 2009 survey, and 29.5°N, 30.5°N, and 32.5°N during the 2015 survey, with no successful trawl in 2011. The locations of successful trawls are marked as red circles with yellow edges on Fig. 2. The 2009 trawls were conducted to sample both the nighttime SSL and the daytime DSL, typically from the surface to ~200-m and roughly between 400 and 800-m depth, respectively. All trawls during the 2015 surveys were limited to nighttime SSL. There was one trawl per latitude and layer except for the 32°N and 36°N latitudes during 2009, where there were two successful trawls for each layer. The number of successful trawls allowed for eleven trawl samples to be analyzed overall with no repetitions of sampling except for one repetition at two stations in 2009.

Trawl samples were separated onboard into four basic groups by scattering characteristics: fish (predominantly with gas-bladder), squid, shrimp-like crustaceans, and gelatinous (predominantly without gas-inclusions). Wet volumes were measured and weighted by approximated volume sampled, estimated as 30-min fishing times. Due to severe limitations of sample size, latitudinal positions of sampling especially during 2015, the lack of our ability to separate samples from specific depths and times, as well as inherent biases in trawl data caused by selectivity of nets and avoidance behavior of organisms (Boersch-Supan et al., 2017; De Robertis et al., 2017; Pakhomov et al., 2010; Suntsov et al., 2010), trawl data were only used as simple guides to relative compositions to help interpret the acoustics data.

2.3. Statistical analyses

The effects of the STF and TZCF on NASC, as well as the relationships between various environmental variables and NASC were assessed using generalized linear models (GLM) and analysis of variance (ANOVA). Given that this study serves as first investigation of the region with complex variables that can have profound effects on micronekton distribution and composition, the linear model was chosen in an effort to help conceptualize the results. Since NASC EDSUs could potentially be spatiotemporally autocorrelated, the independence of observations (EDSUs) were assured by confirming random patterns of the model residuals along the surveys and ensuring the absence of autocorrelations of residuals at the 95% confidence level. Examples of residual plots showing spatially random patterns as well as their insignificant autocorrelations are shown in Supplementary Materials Figs. S1 and S2.

NASC values' dependence on the distance from the fronts over each layer (water-column, SSL, and DSL) and at all available frequencies were assessed by the model NASC $\sim D_{STF} + D_{TZCF}$, where D_{STF} and D_{TZCF} denote the distances to the positions of the fronts, P_{STF} and P_{TZCF}, respectively. NASC values were also modelled from temperature, Chl-a, and oxygen, as NASC ~ Temp + Chl-a + Oxy. Temperature and oxygen values were averaged over the appropriate NASC layer while Chl-a were calculated as the upper 150 m integrated values for the model.

In addition of obtaining information on the relationships of NASC to distances to the fronts and to environmental variables, the effects of varying environmental conditions and variability among surveys were assessed using N-way ANOVA. The meridional Regions were defined as the Subtropical Gyre ($\geq 26N^{\circ}$ & $\leq P_{STF} - 0.5^{\circ}$), STF Region ($P_{STF} \pm 0.5^{\circ}$), TZCF Region ($P_{TZCF} \pm 0.5^{\circ}$), and North of TZCF Region ($\geq P_{TZCF} + 0.5^{\circ}$), where P_{STF} and P_{TZCF} denote the positions of the STF and TZCF, respectively. To compare the mean NASC values from the four meridional Regions and from the four Surveys, Regions and Surveys were used as categorical groups in the N-way ANOVA (NASC ~ {Regions, Surveys}). The significance of the Regions and Surveys to the mean NASC were established by multiple pairwise comparison tests performed on the group means.

3. Results

3.1. The environment

In situ salinities (and temperatures) show the estimated position of the STF at 31.00°N, 32.00°N, 32.00°N, and 30.50°N in the spring of 2009, 2011 north- and southbound, and 2015, respectively (Fig. 3 top panels and Table 1). *In situ* Chl-a gave estimated positions of the TZCF at 35.50°N for the 2009 northbound and at 32.00°N and 33.75°N for the 2011 north- and southbound transects (Fig. 3, bottom panels and Table 1). The 2015 position of the TZCF could not be determined unequivocally as only the two northernmost contiguous positions (32.25 and 32.50°N) were $\geq$0.2 mg m^{-3} in the upper 20 m (indicated by the dotted lines in Fig. 3*b*). Dissolved oxygen concentrations increased to the north with oxygen fronts approximately at the positions of the STF, with additional increased concentrations near the TZCF (Fig. 3*b*, top panels). The mean depth of the 20 °C isotherm along latitudes south of the STF, used as proxy for the mixed layer depth (MLD), were approximately 180, 150, 120, and 30 m during the four transects, shallowing to the north.

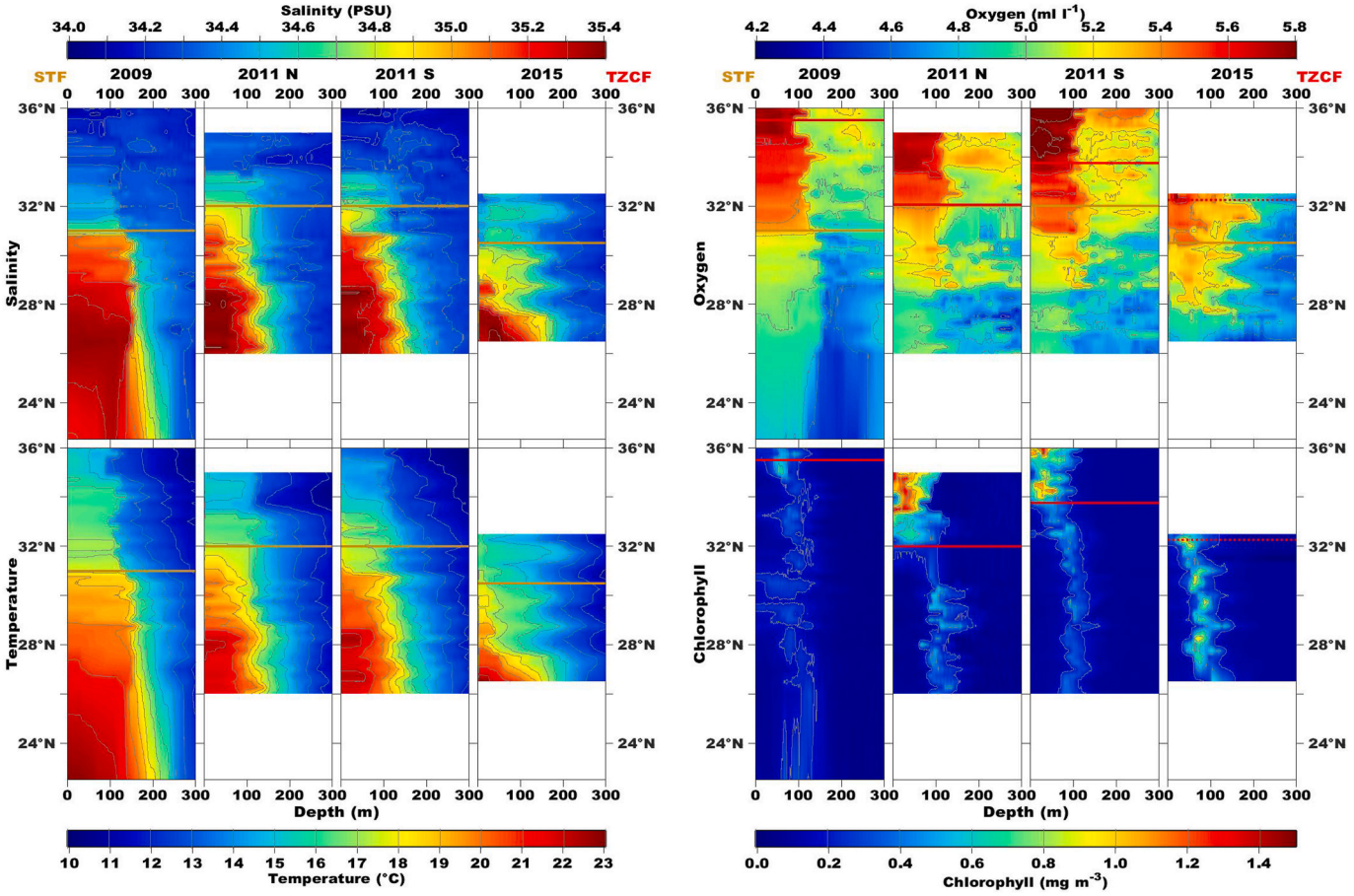

Fig. 3. Salinity (top left), temperature (bottom left), dissolved oxygen (top right), and Chl-a (bottom right) in the upper 300 m along the (left to right) 2009, 2011 northbound, 2011 southbound, and 2015 transects. Beige and red lines show the estimated positions of the STF and TZCF, respectively. The dotted lines on the 2015 Chl-a and oxygen panels indicate that the position of the TZCF was established by only two contiguous $\geq$0.2 mg m^{-3} readings. Note that during the 2011 northbound transect, data south and north of 32°N were obtained along the 158°N and 161°N meridionals.

Table 1
Positions of the fronts, SST (°C) and surface Chl-a (SChl in mg m^{-3}) minimum and maximum, the mean depth (m) of the 20 °C isotherm (proxy for MLD in the Subtropical Gyre Region), as well as integrated 150 m Chl-a for each Survey, as calculated from the CTD data. Surface values are calculated as the upper 20 m means.

	P_{STF}	P_{TZCF}	SST_{min}	SST_{max}	$20°C_{depth}$	$SChl_{min}$	$SChl_{max}$	Chl_{tot}
2009 N	31°00'	35°30'	16.7	21.5	180	0.07	0.25	27.00
2011 N	32°00'	32°00'	16.9	22.2	150	0.06	1.42	39.95
20011 S	32°00'	33°45'	16.52	22.6	120	0.10	1.12	37.48
2015 S	30°30'	–	15.9	23.5	30	0.11	0.33	42.90

The MLD showed a strong negative correlation with the SST in the Subtropical Gyre with a Pearson correlation coefficient of $r = -0.87$ and $p < 0.01$. Overall, the 2015 Survey showed the warmest maximum and coolest minimum SST, calculated as the upper 20 m means, among the Surveys. 2015 also showed the highest upper 150 m integrated Chla values but had the second to the lowest surface Chl-a maximum (Table 1).

On a larger scale, monthly satellite SST and surface Chl-a maps show the meandering SST isotherms primarily in a zonal direction, while the isopleths of Chl-a show a southwest-northeast slope (Fig. 2). Visual inspection of these plots reveal interannual differences with the furthermost extent of cool and warm SST from the north and south during the 2015 Survey, corresponding to the *in situ* data. However, during the 2015 Survey, monthly sea-surface Chl-a concentrations showed exceptionally low values over a large area toward the south, in contrast to those of the *in situ* data.

3.2. Micronekton characteristics

Acoustic backscatter for transects with corresponding *in situ* environmental data are displayed in Fig. 4. The SSL typically occupied the upper 250–300 m, exhibiting strong diel variability in density and vertical extent, while the more permanent DSL was positioned between 400 and 900 m. Ubiquitous DVM between the two layers were clearly visible as well as evidence of vertical migration from the DSL to lower depths, most prominent during the 2015 transect (Fig. 4, bottom panel). While the SSL was typically composed of a single layer, the DSL tended to form two prominent layers at approximately 400–600 and 600–800 m depths, with the deeper DSL being most prominent between ~29 and 35°N. The strong diel variability in the strength of the SSL and the more permanent DSL is clearly illustrated in Fig. 5*a* and *b*, although the boxplots indicate notable differences between the daytime and nighttime DSL NASC. Since regional patterns in the strength of micronekton backscatter and its relative changes from survey to survey were relatively consistent among

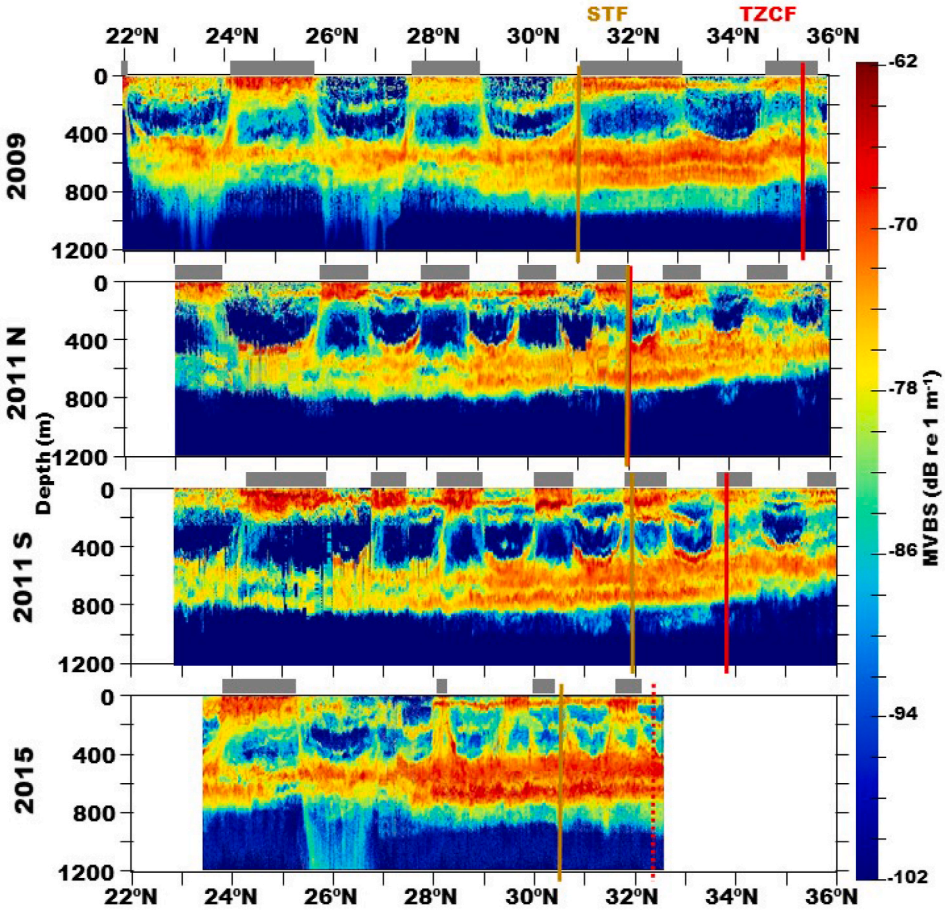

Fig. 4. MVBS, proxy for density, from the 4 transects with *in situ* CTD data in the upper 1200 m at 38 kHz. Gray shaded areas above panels indicate nighttime. Positions of the STF and TZCF are indicated by the beige and red vertical lines, respectively.

all frequencies, Fig. 5 shows only the 38 kHz values for simplicity. See Fig. S3 in the Supplementary Materials for 70 kHz and 120 kHz values for the SSL and DSL.

All surveys had significantly higher water-column NASC marginal means in the STF Region than at any other region, including the TZCF (Fig. 6*a* and Table 2). Given that most of the biomass is within the DSL both day and nighttimes, the regional pattern in the water-column NASC was due primarily to the pattern of the DSL (Fig. 5). NASC in the STF was significantly higher than in all other regions with the exception of the nighttime SSL in the Subtropical Gyre (Table 2*b*), due to exceptionally high NASC values during the 2011S survey. The positive influence of STF on backscatter is confirmed by the ANOVA results on the GLM NASC ~ $D_{STF} + D_{TZCF}$, showing a significant negative relationship between distance from the STF and water-column and DSL NASC at both available frequencies (Table 3). The relationship between the TZCF was not significant at 38 kHz and only showed a positive relationship at the 70 kHz (Table 3). The SSL showed no significant relationship with distance to either fronts at the 38 kHz and a positive relationships with the STF at the 70 and 120 kHz. Fig. 7 provides a visual representation of the effects of the STF on 38 kHz NASC in the water-column and the DSL but showing no apparent relationship of the SSL NASC values with distance from the STF (see also Table 3).

ANOVA on the relationships of NASC and temperature, Chl-a, and oxygen concentrations, (NASC ~ Temp + Chl-a + Oxy) revealed the general importance of temperature to NASC, while the effects of Chl-a and oxygen concentrations on NASC were mostly insignificant (Table 4). Temperature showed mostly significant positive relationships with NASC. The relationships between Chl-a and NASC were mostly insignificant with the exception of a significant positive relationship with 38 kHz daytime water-column and negative relationships with 70 kHz nighttime water-column and day and nighttime DSL NASC. Oxygen showed no significant relationship with NASC except for the positive relationship with daytime water-column values at both 38 and 70 kHz frequencies (Table 4).

Comparing NASC marginal means among Surveys, the 2015 values were significantly higher than those from any of the other surveys in the water-column and the DSL (Fig. 6*b* and Table 2). No other Survey showed significantly different marginal means from all other surveys for these layers. Note that the insignificant differences in the nighttime NASC values in the SSL between the 2015 and 2011S Surveys (Table 2*b*) did not degrade the significance of the higher 2015 total (water-column) nighttime NASC values relative to those during 2011S. To ensure that these results are not biased by the lack of data in the 2015 Survey from the two regions with relatively low NASC values (TZCF and North of TZCF), the N-way ANOVA NASC ~ {Regions, Surveys} were recalculated using data only from the two Regions that could be sampled over all four Surveys. These analyses show no significant changes in the results (see equivalents of Fig. 6 and Table 2 in Supplementary Materials Fig. S4 and Table S1).

While the regional patterns in the strength of micronekton backscatter were relatively consistent among all frequencies and among Surveys, apparent differences between the relative contributions of frequencies were observed (Fig. 8). In general, differences between frequencies (δ dB, defined as 70-38 kHz, 120-38 kHz, and 120-70 kHz MVBS) were higher at the STF and to its north than in the Subtropical Gyre Region, indicating differing composition of the layers between south and north of the STF. In addition, the 2009 and 2011 δdB values were all negative, while the mean 2015 δdB values were significantly

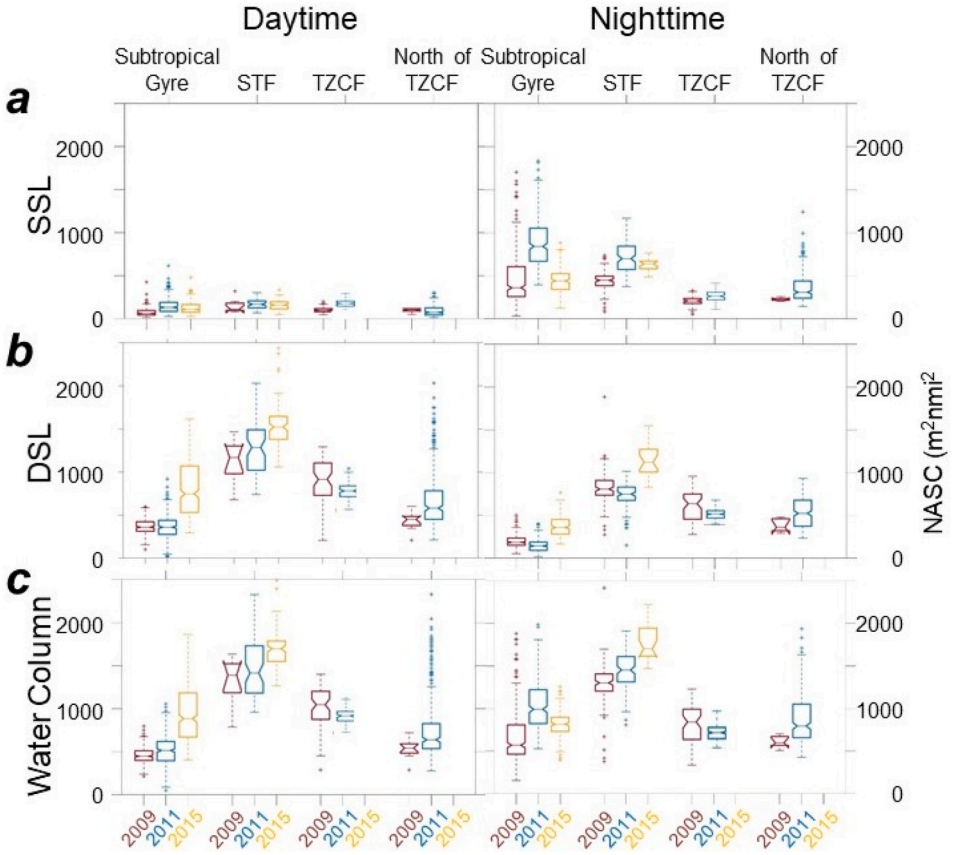

Fig. 5. Daytime (left) and nighttime (right) NASC, proxy for relative biomass of the *(a)* SSL, (*b*) DSL, and (*c*) the total water-column at the 38 kHz frequency. 2011 values are calculated from averaged northbound and southbound data. Boxes represent the first, second, and third quartile of the medians, with notches indicating the 95% confidence intervals. Individual points considered outliers are marked with the '+' symbol.

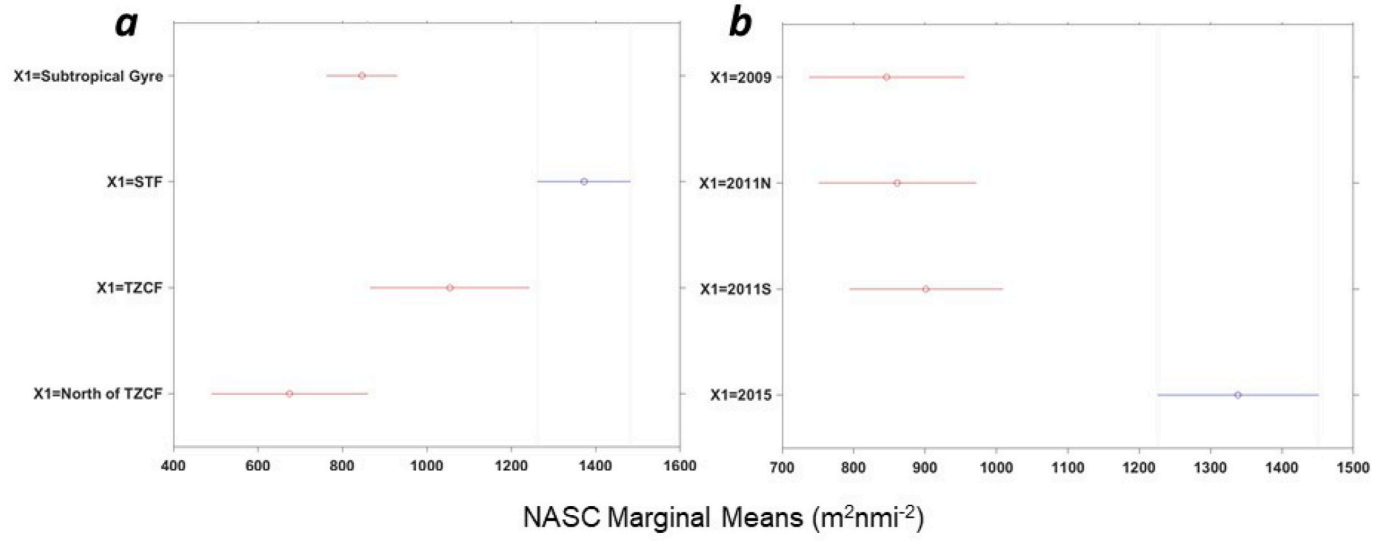

Fig. 6. Water-column NASC marginal means of Regions (left) and Surveys (right) with 95% confidence intervals obtained from the multiple pairwise comparison tests NASC ~ {Regions, Surveys}.

higher at 95% confidence, reaching positive δdB in the DSL (Fig. 8).

In contrast to the general pattern of increased NASC values at STF latitudes for the layers sampled, trawl sample volumes generally increased from south to north, with highest values at the northernmost latitudes for all surveys (Table 5). Percent composition of catch in 2009 was highest for fish at 26°N & 32°N and for gelatinous organisms at 36°N. During 2015, however, gelatinous organisms overwhelmingly dominated the catch at all latitudes. Percent contribution also differed markedly for crustaceans between 2009 and 2015. During the 2009 trawls, sizes of gelatinous organisms and squids were noted to increase with latitude.

Table 2
NASC marginal means with their standard errors (*a*) and 95% *p*-values (*b*), obtained from the multiple pairwise comparison tests on NASC ~ {Regions, Surveys}. Significant *p*-values at the 95% are in bold.

(a)

	Day WC		Night WC		Day DSL		Night SSL	
	Mean	**SE**	**Mean**	**SE**	**Mean**	**SE**	**Mean**	**SE**
Regions								
Subtropical Gyre	845.81	38.59	1077.78	42.38	683.25	35.26	547.53	29.96
STF	1372.16	56.89	1510.19	61.20	1185.92	51.98	572.49	43.26
TZCF	1054.22	99.39	697.17	88.97	826.56	90.81	119.21	62.89
North of TZCF	675.10	96.52	1054.34	118.25	583.98	88.19	250.95	83.59
Surveys								
2009	846.29	63.61	715.41	69.58	723.64	58.76	134.47	49.19
2011N	861.15	61.24	1002.95	57.45	737.69	56.57	471.96	40.61
2011S	901.22	60.33	1193.53	61.17	744.71	55.73	626.58	43.24
2015	1338.63	69.66	1477.59	93.93	1207.83	64.35	257.16	66.40

(b)

		p-values			
		Day WC	Night WC	Day DSL	Night SSL
Region 1	**Region 2**				
STF	Subtropical Gyre	**0.00**	**0.00**	**0.00**	0.96
STF	TZCF	**0.04**	**0.00**	**0.01**	**0.00**
STF	North of TZCF	**0.00**	**0.01**	**0.00**	**0.01**
TZCF	Subtropical Gyre	0.22	**0.00**	0.46	**0.00**
North of TZCF	Subtropical Gyre	0.36	1.00	0.72	**0.01**
North of TZCF	TZCF	**0.04**	0.07	0.22	0.55
Survey 1	**Survey 2**				
2015	2009	**0.00**	**0.00**	**0.00**	**0.00**
2015	2011N	**0.00**	**0.00**	**0.00**	**0.02**
2015	2011S	**0.00**	**0.04**	**0.00**	0.34
2011N	2009	1.00	**0.01**	1.00	**0.00**
2011S	2009	0.91	**0.00**	0.99	**0.00**
2011S	2011N	0.96	0.09	1.00	**0.04**

Table 3
ANOVA results on GLM for the relationship between NASC and distances to the STF and TZCF. Significant *p*-values at the 95% are in bold.

		WC			SSL			DSL		
		tTest	F	*p*	tTest	F	*p*	tTest	F	*p*
38 kHz	**STF**	−2.45	6.01	**0.02**	0.74	0.55	0.46	−6.13	37.53	**0.00**
	TZCF	0.39	0.16	0.69	1.11	1.24	0.27	−1.40	1.95	0.17
70 kHz	**STF**	−3.09	4.93	**0.00**	2.39	5.70	**0.02**	−5.55	30.77	**0.00**
	TZCF	5.29	0.57	**0.00**	1.55	2.41	0.12	4.11	16.91	**0.00**
120 kHz	**STF**	–	–	–	2.22	4.93	**0.03**	–	–	–
	TZCF	–	–	–	0.76	0.57	0.45	–	–	–

4. Discussion

The results of this study indicate that the STF had a significant positive effect on the relative biomass of micronekton and acted as a boundary for the distribution of specific micronekton taxonomic groups, displaying the typical characteristics of an ecotone (e.g., Kark and van Rensburg, 2006). Water-column NASC marginal means were significantly higher at the STF Region than any of the other regions at all frequencies, indicating that the increase was at least partially due to an increase in relative biomass of organisms. The observed decrease in relative biomass with northward distance from the STF is in agreement with the positive relationship found between temperature and NASC values, a somewhat unexpected result based on the general assumption that warm temperatures are typically associated with oligotrophic regions depleted of nutrients (e.g., Gnanadesikan et al., 2011; Polovina et al., 2008) leading to decreased biomass of higher trophic level organisms based on bottom-up forcing. However, the present study found no evidence of an effect of chlorophyll concentrations on micronekton biomass, but the results are in agreement with previous studies indicating a positive effect of the convergence at fronts (e.g., Béhagle et al., 2014; Domokos, 2009; Lehodey, 2001; Lima, 2002). Higher micronekton biomass associated with warmer temperatures is also reported by other studies (Béhagle et al., 2016; e.g., Fennell and Rose, 2015), and it could be due to differences in other hydrographic characteristics associated with changes in water masses with differing temperatures. For example, a study showed that relatively warm water masses carried by the South Equatorial Counter Current contained significantly higher micronekton biomass than the surrounding cooler South Equatorial Current waters in the southwest Pacific, likely the result of differences in hydrographic and/or biogeochemical conditions downstream (Domokos, 2009).

The delineation of species distribution by the STF, as indicated by the δdB values, have been shown by other studies at different water-mass boundaries and at thermohaline fronts (e.g., Pearcy, 1991). Further, Brinton (1962) found specific euphausiid species almost exclusively occurring either in subtropical waters or in the North Pacific Transition Zone. In this study, the generally higher δdB values north of the STF relative to its south are in agreement with lower percent biomass of fish

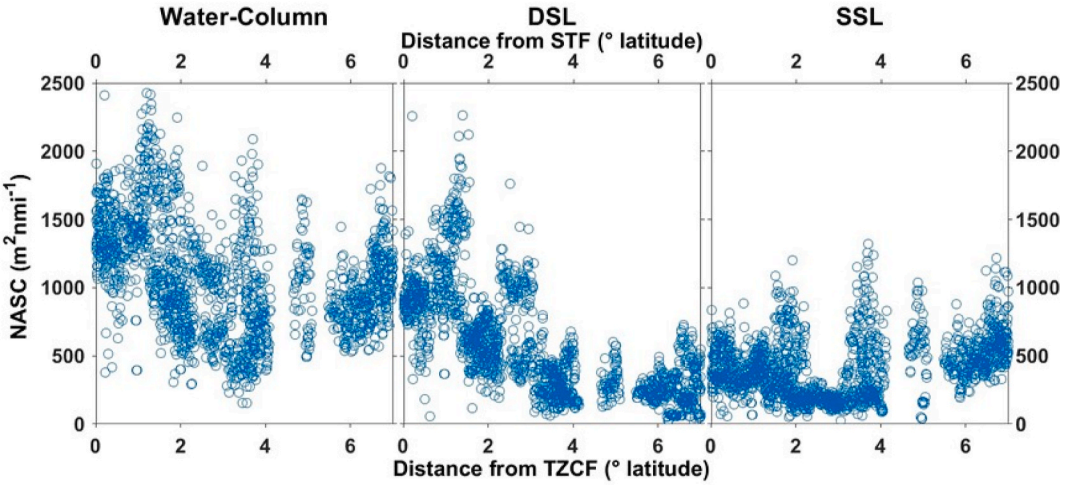

Fig. 7. Scatterplots of distances from the STF for the (from left) water-column, DSL, and SSL 38 kHz nighttime NASC.

Table 4
ANOVA on GLM of *in situ* environmental variables with NASC per layer, day and night-times, and at each available frequencies. Significant *p*-values are marked with bold.

		Night WC			Day WC			Night SSL			Night DSL			Day DSL		
		tStsat	F	p	tStsat	F	p	tStsat	F	p	tStsat	F	p	tStsat	F	p
38 kHz	**Temp**	3.78	14.27	**0.00**	0.12	0.01	0.91	3.37	11.36	**0.00**	0.48	0.23	0.64	2.72	7.37	**0.01**
	Chl-a	−0.47	0.23	0.64	3.77	14.19	**0.00**	1.07	1.15	0.29	−0.24	0.06	0.81	−0.66	0.43	0.51
	Oxy	−0.83	0.69	0.41	3.89	15.16	**0.00**	−1.04	1.09	0.31	−1.26	1.59	0.22	0.09	0.01	0.93
70 kHz	**Temp**	2.76	7.63	**0.01**	2.58	6.67	**0.02**	3.49	12.15	**0.00**	1.20	1.45	**0.01**	4.90	23.98	**0.00**
	Chl-a	−3.11	9.65	**0.00**	−1.44	2.09	0.16	1.00	0.99	0.32	−2.26	5.09	**0.03**	−4.32	18.64	**0.00**
	Oxy	−0.03	0.00	0.98	3.35	11.25	**0.00**	−0.76	0.57	0.46	−1.03	1.05	0.31	0.46	0.21	0.65
120 kHz	**Temp**							3.01	9.09	**0.01**						
	Chl-a							0.94	0.89	0.35						
	Oxy							−0.51	0.26	0.61						

with swim-bladders relative to those of gelatinous organisms and shrimp-like crustaceans at the northern stations obtained in the trawl catches (e.g., Béhagle et al., 2017; Benoit-Bird and Lawson, 2016; Dornan et al., 2019; Korneliussen and Ona, 2003), a composition change observed in prior studies (Cox et al., 2013). Note that the limited number and unsuitable locations of the net samples, exacerbated by the inability to separate organisms caught by depth and the exact time of fishing, limits the utility of the trawl results to qualitative indications of changes in the relative composition of the SSL and DSL and cannot reflect accurate changes in their relative biomass. Further, trawls can only provide a "limited window of reality" (Merrett et al., 1991) due to their spatiotemporal limitations, rendering comparisons to biomass and composition estimated from the continuous acoustics data problematic. Trawl data have not been found to correlate to acoustics data in most cases (e.g., Donaldson and William, 1972; Irigoien et al., 2014; Sutton, 2013) as they can provide reliable biomass estimates only when predominant species are well sampled by the net (McClatchie et al., 2000), apparently not the case in the present study. Trawls are also known to disproportionally under-sample organisms due to avoidance behavior, limitations imposed by the type and size of net, damage to soft-bodied organisms, and light conditions (Boersch-Supan et al., 2017; De Robertis et al., 2017; Drazen et al., 2011; Kaartvedt et al., 2012). The net used in this study has been shown to better sample micronekton with a bias toward larger sizes relative to two other nets with smaller mouth openings and mesh sizes (Pakhomov et al., 2010; Suntsov et al., 2010). Larger micronekton are likely better able to escape the net, raising further questions regarding the accuracy of trawl-volume estimates.

The lack of a significant effect of chlorophyll concentrations on micronekton biomass, linked via three tropic levels, does not necessarily indicate the lack of bottom-up forcing but could be the result of the highly dynamic environment. It could also be due to seasonal variability in the position of the TZCF (Ayers and Lozier, 2010) and/or lagged effects of environmental conditions on organisms (e.g., Milligan and Sutton, 2020). Thermohaline fronts acting as seasonal boundary for species distribution have previously been observed in other regions (e.g., Menkes et al., 2015; Moku et al., 2003). Hydrographic conditions or processes in nearby environment might also be affecting micronekton in the survey area. For example, Suntsov and Domokos (2013) found influence of the North Equatorial Counter Current on macrozooplankton and micronekton several degrees north from its boundary. It is also important to note that not all micronekton undergo DVM and species that invariably occupy deeper depths are outside the influence of chlorophyll concentrations in the euphotic zone. The observed frequency-dependent variability in scattering layer response to the fronts is likely due to the differences in backscatter properties of non-migratory organisms that exclusively occupy depths of the DSL (and below) or the SSL, and of those that undergo DMV.

The observed positive effect of temperature in combination with the lack of a significant effect of chlorophyll concentrations (and the TZCF) on micronekton could also be due to micronekton responding to large-scale forcing that is masked by meso- or sub-mesoscale variability in the *in situ* chlorophyll data. Meso- or sub-mesoscale forcing in chlorophyll concentrations and the lack of response by micronekton is consistent with the observed variability in the latitudinal position of the TZCF with a corresponding the lack of significant differences in overall micronekton biomasses between the two 2011 Surveys, approximately one week apart (compare Fig. 3 and Table 1 to Table 2*b*). The dominance of meso- or sub-mesoscale variability in the *in situ* chlorophyll

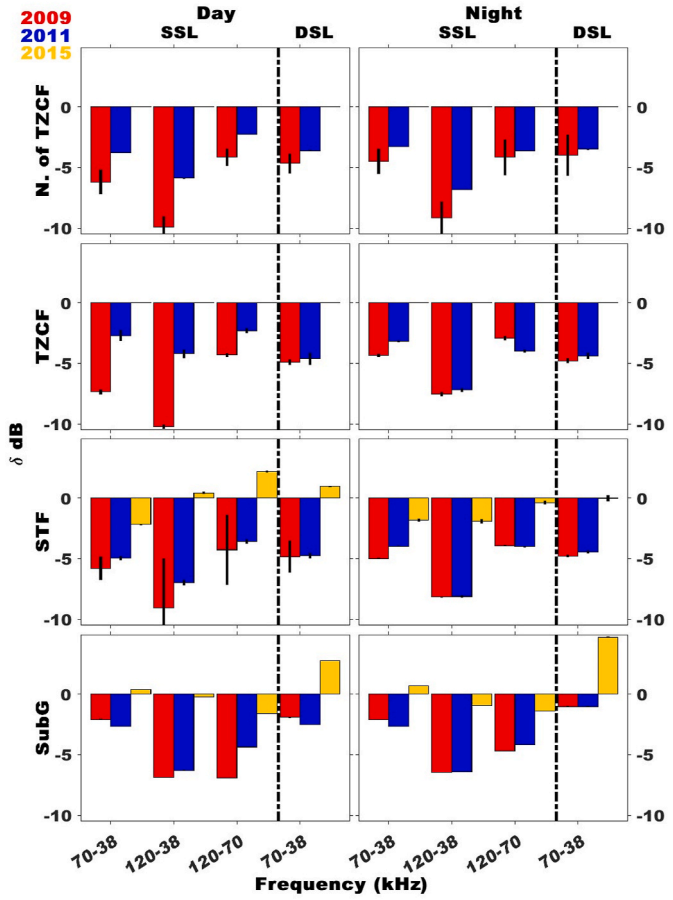

Fig. 8. δdB values during the 2009 (red), 2011 (blue), and 2015 (yellow) transects, separate by day (left panels) and night (right panels) at the four regions defined by the positions of the fronts from south to north represented from bottom to top plots. Note that the 2015 values for the TZCF and North of TZCF regions are not available since the 2015 survey did not reach the TZCF according to the *in situ* data.

Table 5
Total wet volumes (V in dl per 30 min, left) and percent contributions from the four major groups of organisms for the 2009 daytime DSL (top), 2009 nighttime SSL (middle), and 2015 nighttime SSL (bottom) trawls at the three meridional positions with available data. Trawl positions are as indicated on Fig. 2 by yellow-edged red circles.

			Total Wet Volume (dL)	% Fish	% Squid	% Crust.	% Gelatinous
2009	**DSL**	26°00′N	3.62	48.72	10.26	25.64	15.38
		32°00′N	5.44	55.04	5.29	25.43	14.24
		36°00′N	11.31	19.99	1.28	10.84	67.89
	SSL	26°00′N	13.40	63.41	9.76	17.07	9.76
		32°00′N	5.50	51.72	22.41	20.69	5.17
		36°00′N	45.89	6.49	2.07	5.24	86.20
2015	**SSL**	29°15′N	3.52	28.72	17.05	0.96	53.28
		30°30′N	6.10	9.82	8.98	0.97	80.23
		32°30′N	7.47	7.22	11.96	3.23	77.59

concentrations is further indicated by the apparent inconsistencies between the *in situ* and monthly satellite surface chlorophyll concentrations during the Surveys: on the lager-scale, surface chlorophyll concentrations were lowest during the 2015 Survey (Fig. 2, bottom panels), while *in situ* data showed the highest surface chlorophyll concentrations (Table 1). The importance of mesoscale forcing on the meridional position of the TZCF, in addition of largescale influences (Qiu and Chen, 2011), is postulated by Howell et al. (2017).

The hypothesis that micronekton respond partially to largescale forcing is supported by the observed significantly higher micronekton biomass (Fig. 6*b* and Table 2) and changed composition (Fig. 8) during the 2015 Survey relative to those of the other Surveys. The changes in 2015 hydrological observations relative to those of the other Surveys are consistent with the expected effects of the 2014–2017 extreme warming event, the "Blob" (Bond et al., 2015; Newman et al., 2016). The highest maximum SST, as shown by the monthly satellite data (Fig. 2, top panels), corroborated by *in situ* temperatures (Table 1), the largest extent of the highly oligotrophic area observed in the monthly satellite data (Fig. 2, bottom panels), and the shallowest MLD (Table 1) during 2015 are all the expected signatures of the Blob (Amaya et al., 2016, 2021; Bond et al., 2015; Eakin et al., 2017; Khangaonkar et al., 2021; Newman et al., 2016). Note that the lowest SST_{min} during the 2015 Survey (Fig. 2 top panels and Table 1) apparently reflects the strong Aleutian low extending furthest to the south during the 2015 strong positive Pacific Decadal Oscillation phase. However, note that the 2015 Survey was conducted approximately 2.5 weeks later in the year than the other three Surveys, potentially contributing to the marked differences in micronekton characteristics during that year. Phenology can also vary on an inter-annual scale, adding another possible source for the differences. The horizontal distribution patterns in the *in situ* and satellite SST at the location of the Surveys are in agreement with concurrent 2015 SST anomaly (SSTA) values (maps and data available from NOAA CoastWatch at https://coastwatch.pfeg.noaa.gov/erddap/griddap/erdAGtanmmday.graph) that indicate positive basin-scale SSTA with negative values along the 158°W meridian (not shown). However, during preceding months the SSTA in the survey area was positive, in result of the furthest expansion of the Blob to the west (Amaya et al., 2016; Bond et al., 2015; Peterson et al., 2014, 2016) that moved to the east by the April 2015 survey. The observed δdB and trawl results are in agreement with a previous study that found significant increase in gelatinous micronekton, and in some instances cephalopod biomass as well as an overall increase in diversity in response to the 2014–2017 heat-wave in the Eastern North Pacific due to significant differences in pelagic communities further to the west (Brodeur et al., 2019).

Extension of highly oligotrophic regions, such as the Subtropical Gyre (Polovina et al., 2008) and an increase in SST due to reduced vertical mixing and a shoaling of the thermocline leading to shallower MLD (Alexander et al., 2018; Capotondi et al., 2012; Whitney, 2015) are also the in agreement with the signatures of long-term climate change. The observed increase of micronekton biomass with increasing temperature are in agreement of studies indicating that micronekton biomass is expected to increase on a global scale due to climate warming and changes in the ecosystem, especially in the DSL (Proud et al., 2017; Receveur et al., 2021) and in the epipelagic and mesopelagic zones away from the equator (Costello and Breyer, 2017). In addition, the significant increase in δdB during the 2015 Survey relative to the preceding Surveys are also in agreement with size structure studies showing that increased temperatures result in a shift from larger to smaller sizes of organisms and species preference (Daufresne et al., 2009; Sheridan and Bickford, 2011; Woodworth-Jefcoats et al., 2015; Yvon-Durocher et al., 2011), based on the size-dependence of acoustic backscatter at different frequencies (e.g., Lebourges-Dhaussy et al., 2014; Simmonds and MacLennan, 2005). Note that the highest *in situ* upper 150-m integrated chlorophyll concentrations observed in 2015 (Table 1) could have provided the necessary support for the increased micronekton biomass during that year. However, the limited availability of data prevent the assessment of largescale variability or climate modes on micronekton in the region. Further, the results of the present study are contrary to some model predictions (Bryndum-Buchholz et al., 2019; Kwiatkowski et al., 2019; Lefort et al., 2015; Lotze et al., 2019) indicating that based on current knowledge, the effects of largescale variability on micronekton are biomass and compositions are largely uncertain.

5. Conclusions

The seasonally varying STFZ in the central North Pacific aggregates top predators and serves as focus for commercial fishery activities. It is also a region of concern over bycatch of protected species. Top predators are assumed to be drawn to the area by the increased presence of prey, micronekton, which is thought to be the results of increased chlorophyll concentrations in the STFZ. In this study, the presence of increased micronekton biomass was confirmed in the STFZ; however, the increase was associated with another prominent front in the STFZ, the thermohaline STF. The STF was also found to serve as a boundary between species associated with lower-salinity, warmer waters to its south and with the relatively more saline, cooler waters to its north. Chlorophyll concentrations or the meridional position of the TZCF did not show an effect on micronekton relative biomass or composition. On a larger scale, data from this study also corresponds to the expected effects of large marine heatwaves and warming.

As a region where relatively stark changes in contrasting conditions occur over a relatively small geographic distance, the STFZ is expected to exhibit a more dramatic sensitivity to climate variability and change in comparison to the relatively more homogeneous gyres to its north and south. Data from the last few decades indicate that the warm, oligotrophic North Pacific Subtropical Gyre is expanding (Polovina et al., 2008), and the decline in primary productivity with warming temperatures is predicted to result in a decline in top predator biomass followed by a similar decline in fisheries performance (e.g., Polovina et al., 2008; Woodworth-Jefcoats et al., 2017). However, based on our current knowledge, it is unclear how climate change will influence the spread of nutrient-poor waters and how this expansion will affect the phenology of target and protected species along the STFZ.

The present study serves as a first insight into the role of the two most prominent fronts within the STFZ, the STF and TZCF, on the relative biomass and composition of micronekton in the central North Pacific. However, future surveys are necessary to understand the mechanisms involved and to confirm the observed effects. Further, development of time series over the STFZ in the central North Pacific are needed to understand the broader effects of mesoscale variability and the effects of largescale events and climate change on this economically important region.

Declaration of competing interest

The authors declare that they have no known competing financial interests or personal relationships that could have appeared to influence the work reported in this paper.

Data availability

All data used in this study is publicly available with links provided

Acknowledgements

The author acknowledges the help and support of many who made this project possible. I thank the officers, crew, and scientific party of the NOAA Ship *Oscar Elton Sette* for their help and dedication to make this study possible. I especially thank Amy Comer and Aimee Hoover for their help in cleaning acoustic backscatter data from the 2009 and 2011 Surveys. I thank Evan Howell and Phoebe Woodworth-Jefcoats for their assistance with CTD casts and *in situ* Chl-a calculations, and Justin Suca for his invaluable support with statistical methodology. The author thanks scientific staff at the Pacific Islands Fisheries Science Center, especially Ryan Rykaczewski for providing valuable suggestions and insights, Evan Howell for engaging in beneficial discussions at the early stages of this project, and to Phoebe Woodworth-Jefcoats for reviewing an early version of this manuscript.

Appendix A. Supplementary data

Supplementary data to this article can be found online at https://doi.org/10.1016/j.dsr.2023.104076.

References

Alexander, M.A., Scott, J.D., Friedland, K.D., Mills, K.E., Nye, J.A., Pershing, A.J., Thomas, A.C., 2018. Projected Sea Surface Temperatures over the 21st Century: Changes in the Mean, Variability and Extremes for Large Marine Ecosystem Regions of Northern Oceans. Elementa. https://doi.org/10.1525/elementa.191.

Amaya, D.J., Bond, N.E., Miller, A.J., Deflorio, M.J., 2016. The Evolution and Known Forcing Mechanisms behind the 2013-2015 North Pacific Warm Anomalies "A Tale of Two Blobs" in Variations.

Amaya, D.J., Alexander, M.A., Capotondi, A., Deser, C., Karnauskas, K.B., Miller, A.J., Mantua, N.J., 2021. Are long-term changes in mixed layer depth influencing north pacific marine heatwaves? Bull. Am. Meteorol. Soc. 102, S59. https://doi.org/10.1175/BAMS-D-20-0144.1. –S66.

Ayers, J.M., Lozier, M.S., 2010. Physical controls on the seasonal migration of the North Pacific transition zone chlorophyll front. J. Geophys. Res. Oceans 115, 1–11. https://doi.org/10.1029/2009JC005596.

Baker, J.D., Polovina, J.J., Howell, E.A., 2007. Effect of variable oceanic productivity on the survival of an upper trophic predator, the Hawaiian monk seal Monachus schauinslandi. Mar. Ecol. Prog. Ser. 346, 277–283. https://doi.org/10.3354/meps06968.

Béhagle, N., Du Buisson, L., Josse, E., Lebourges-Dhaussy, A., Roudaut, G., Ménard, F., 2014. Mesoscale features and micronekton in the Mozambique Channel: an acoustic approach. Deep Sea Res 2 Top Stud Oceanogr 100, 164–173. https://doi.org/10.1016/j.dsr2.2013.10.024.

Béhagle, N., Cotté, C., Ryan, T.E., Gauthier, O., Roudaut, G., Brehmer, P., Josse, E., Cherel, Y., 2016. Acoustic micronektonic distribution is structured by macroscale oceanographic processes across 20-50°S latitudes in the South-Western Indian Ocean. Deep Sea Res 1 Oceanogr Res Pap 110, 20–32. https://doi.org/10.1016/j.dsr.2015.12.007.

Béhagle, N., Cotté, C., Lebourges-Dhaussy, A., Roudaut, G., Duhamel, G., Brehmer, P., Josse, E., Cherel, Y., 2017. Acoustic distribution of discriminated micronektonic organisms from a bi-frequency processing: the case study of eastern Kerguelen oceanic waters. Prog. Oceanogr. 156, 276–289. https://doi.org/10.1016/j.pocean.2017.06.004.

Benoit-Bird, K.J., Lawson, G.L., 2016. Ecological insights from pelagic habitats acquired using active acoustic techniques. Ann. Rev. Mar. Sci 8, 463–490. https://doi.org/10.1146/annurev-marine-122414-034001.

Benoit-Bird, K.J., Zirbel, M.J., McManus, M.A., 2008. Diel variation of zooplankton distributions in Hawaiian waters favors horizontal diel migration by midwater micronekton. Mar. Ecol. Prog. Ser. 367, 109–123. https://doi.org/10.3354/meps07571.

Benoit-Bird, K.J., Southall, B.L., Moline, M.A., 2016. Predator-guided sampling reveals biotic structure in the bathypelagic. Proc. Biol. Sci. 283, 20152457 https://doi.org/10.1098/rspb.2015.2457.

Block, B.A., Jonsen, I.D., Jorgensen, S.J., Winship, A.J., Shaffer, S.A., Bograd, S.J., Hazen, E.L., Foley, D.G., Breed, G.A., Harrison, A.L., Ganong, J.E., Swithenbank, A., Castleton, M., Dewar, H., Mate, B.R., Shillinger, G.L., Schaefer, K.M., Benson, S.R., Weise, M.J., Henry, R.W., Costa, D.P., 2011. Tracking apex marine predator movements in a dynamic ocean. Nature 475, 86–90. https://doi.org/10.1038/nature10082.

Boersch-Supan, P.H., Rogers, A.D., Brierley, A.S., 2017. The distribution of pelagic sound scattering layers across the southwest Indian Ocean. Deep Sea Res 2 Top Stud Oceanogr 136, 108–121. https://doi.org/10.1016/j.dsr2.2015.06.023.

Bograd, S.J., Foley, D.G., Schwing, F.B., Wilson, C., Laurs, R.M., Polovina, J.J., Howell, E. A., Brainard, R.E., 2004. On the seasonal and interannual migrations of the transition zone chlorophyll front. Geophys. Res. Lett. 31, 1–5. https://doi.org/10.1029/2004GL020637.

Bond, N.A., Cronin, M.F., Freeland, H., Mantua, N., 2015. Causes and impacts of the 2014 warm anomaly in the NE Pacific. Geophys. Res. Lett. 42, 3414–3420. https://doi.org/10.1002/2015GL063306.

Brinton, E., 1962. The Distribution of Pacific Euphausiids. Bulletin of the Scripps Institution of Oceanography.

Brodeur, R., Yamamura, O., 2005. Micronekton of the North pacific. PICES Scientific Report No 30 30, 1–115.

Brodeur, R.D., Seki, M.P., Pakhomov, E. a, Suntsov, A.V., 2005. Micronekton - what are they and why are they important. PICES Press 13, 7–11.

Brodeur, R.D., Auth, T.D., Phillips, A.J., 2019. Major shifts in pelagic micronekton and macrozooplankton community structure in an upwelling ecosystem related to an unprecedented marine heatwave. Front. Mar. Sci. 6, 1–15. https://doi.org/10.3389/FMARS.2019.00212.

Bryndum-Buchholz, A., Tittensor, D.P., Blanchard, J.L., Cheung, W.W.L., Coll, M., Galbraith, E.D., Jennings, S., Maury, O., Lotze, H.K., 2019. Twenty-first-century climate change impacts on marine animal biomass and ecosystem structure across ocean basins. Global Change Biol. 25, 459–472. https://doi.org/10.1111/gcb.14512.

Capotondi, A., Alexander, M.A., Bond, N.A., Curchitser, E.N., Scott, J.D., 2012. Enhanced upper ocean stratification with climate change in the CMIP3 models. J. Geophys. Res. Oceans 117. https://doi.org/10.1029/2011JC007409.

Cascão, I., Domokos, R., Lammers, M.O., Santos, R.S., Silva, M.A., 2019. Seamount effects on the diel vertical migration and spatial structure of micronekton. Prog. Oceanogr. 175, 1–13. https://doi.org/10.1016/j.pocean.2019.03.008.

Choy, A.C., Wabnitz, C.C.C., Weijerman, M., Woodworth-Jefcoats, P.A., Polovina, J.J., 2016. Finding the way to the top: how the composition of oceanic mid-trophic micronekton groups determines apex predator biomass in the central North Pacific. Mar. Ecol. Prog. Ser. 549, 9–25. https://doi.org/10.3354/meps11680.

Costello, M.J., Breyer, S., 2017. Ocean depths: the mesopelagic and implications for global warming. Curr. Biol. 27, R36–R38. https://doi.org/10.1016/j.cub.2016.11.042.

Cox, M.J., Letessier, T.B., Brierley, A.S., 2013. Zooplankton and micronekton biovolume at the Mid-Atlantic Ridge and Charlie-Gibbs Fracture Zone estimated by multi-frequency acoustic survey. Deep Sea Res 2 Top Stud Oceanogr 98, 269–278. https://doi.org/10.1016/j.dsr2.2013.07.020.

Daufresne, M., Lengfellner, K., Sommer, U., 2009. Global warming benefits the small in aquatic ecosystems. Proc. Natl. Acad. Sci. USA 106, 12788–12793. https://doi.org/10.1073/pnas.0902080106.

de Robertis, A., McKelvey, D.R., Ressler, P.H., 2010. Development and application of an empirical multifrequency method for backscatter classification. Can. J. Fish. Aquat. Sci. 67, 1459–1474. https://doi.org/10.1139/F10-075.

De Robertis, A., Taylor, K., Williams, K., Wilson, C.D., 2017. Species and size selectivity of two midwater trawls used in an acoustic survey of the Alaska Arctic. Deep Sea Res 2 Top Stud Oceanogr 135, 40–50. https://doi.org/10.1016/j.dsr2.2015.11.014.

Demer, D.A., Berger, L., Bernasconi, M., Bethke, E., Boswell, K., Chu, D., Domokos, R., 2015. Calibration of acoustic instruments. ICES CRR 133.

Domokos, Réka, 2009. Environmental effects on forage and longline fishery performance for albacore (Thunnus alalunga) in the American Samoa Exclusive Economic Zone. Fish. Oceanogr. 18, 419–438. https://doi.org/10.1111/j.1365-2419.2009.00521.x.

Domokos, R., Seki, M.P., Polovina, J.J., Hawn, D.R., 2007. Oceanographic investigation of the American Samoa albacore (Thunnus alalunga) habitat and longline fishing grounds. Fish. Oceanogr. 16, 555–572. https://doi.org/10.1111/j.1365-2419.2007.00451.x.

Donaldson, H.A., William, G.P., 1972. Sound-scattering layers in the northeastern Pacific. J. Fish. Res. Board Can. 29, 1419–1423.

Doray, M., Josse, E., Gervain, P., Reynal, L., Chantrel, J., 2007. Joint use of echosounding, fishing and video techniques to assess the structure of fish aggregations around moored Fish Aggregating Devices in Martinique (Lesser Antilles). Aquat. Living Resour. 20, 357–366. https://doi.org/10.1051/alr:2008004.

Dornan, T., Fielding, S., Saunders, R.A., Genner, M.J., 2019. Swimbladder morphology masks Southern Ocean mesopelagic fish biomass. Proc. Biol. Sci. 286 https://doi.org/10.1098/rspb.2019.0353.

Drazen, J.C., De Forest, L.G., Domokos, R., 2011. Micronekton abundance and biomass in Hawaiian waters as influenced by seamounts, eddies, and the moon. Deep Sea Res 1 Oceanogr Res Pap 58, 557–566. https://doi.org/10.1016/j.dsr.2011.03.002.

D'Elia, M., Warren, J.D., Rodriguez-Pinto, I., Sutton, T.T., Cook, A., Boswell, K.M., 2016. Diel variation in the vertical distribution of deep-water scattering layers in the Gulf of Mexico. Deep Sea Res 1 Oceanogr Res Pap 115, 91–102. https://doi.org/10.1016/j.dsr.2016.05.014.

Eakin, C.M., Liu, G., Gomez, A.M., De La Cour, J.L., Heron, S.F., Skirving, W.J., Geiger, E. F., Tirak, K.V., Strong, A.E., 2017. Global coral bleaching 2014-2017; status and an appeal for observations. Reef Encount. 31, 20–26.

Escobar-Flores, P., O'Driscoll, R.L., Montgomery, J.C., 2013. Acoustic characterization of pelagic fish distribution across the South Pacific Ocean. Mar. Ecol. Prog. Ser. 490, 169–183. https://doi.org/10.3354/meps10435.

Escobar-Flores, P.C., Décima, M., O'Driscoll, R.L., Ladroit, Y., Roberts, J., 2022. Multiple sampling methods to develop indices of mid-trophic levels abundance in open ocean ecosystems. Limnol Oceanogr. Methods. https://doi.org/10.1002/lom3.10522.

Fennell, S., Rose, G., 2015. Oceanographic influences on deep scattering layers across the North Atlantic. Deep Sea Res 1 Oceanogr Res Pap 105, 132–141. https://doi.org/10.1016/j.dsr.2015.09.002.

Fernandes, 2005. Species Identification Methods from Acoustic Multi-Frequency Information, Sinfami, Final Report.

Gnanadesikan, A., Dunne, J.P., John, J., 2011. What ocean biogeochemical models can tell us about bottom-up control of ecosystem variability. ICES (Int. Counc. Explor. Sea) J. Mar. Sci. 68, 1030–1044. https://doi.org/10.1093/icesjms/fsr068.

Green, D.B., Bestley, S., Trebilco, R., Corney, S.P., Lehodey, P., McMahon, C.R., Guinet, C., Hindell, M.A., 2020. Modelled mid-trophic pelagic prey fields improve understanding of marine predator foraging behaviour. Ecography 43, 1014–1026. https://doi.org/10.1111/ecog.04939.

Hazen, E.L., Johnston, D.W., 2010. Meridional patterns in the deep scattering layers and top predator distribution in the central equatorial Pacific. Fish. Oceanogr. 19, 427–433. https://doi.org/10.1111/j.1365-2419.2010.00561.x.

Hazen, E.L., Jorgensen, S., Rykaczewski, R.R., Bograd, S.J., Foley, D.G., Jonsen, I.D., Shaffer, S.A., Dunne, J.P., Costa, D.P., Crowder, L.B., Block, B.A., 2013. Predicted habitat shifts of Pacific top predators in a changing climate. Nat. Clim. Change 3, 234–238. https://doi.org/10.1038/nclimate1686.

Howell, E.A., Kobayashi, D.R., Parker, D.M., Balazs, G.H., Polovina, J.J., 2008. TurtleWatch: a tool to aid in the bycatch reduction of loggerhead turtles Caretta caretta in the Hawaii-based pelagic longline fishery. Endanger. Species Res. 5, 267–278. https://doi.org/10.3354/esr00096.

Howell, E.A., Hoover, A., Benson, S.R., Bailey, H., Polovina, J.J., Seminoff, J.A., Dutton, P.H., 2015. Enhancing the TurtleWatch product for leatherback sea turtles, a dynamic habitat model for ecosystem-based management. Fish. Oceanogr. 24, 57–68. https://doi.org/10.1111/fog.12092.

Howell, E.A., Bograd, S.J., Hoover, A.L., Seki, M.P., Polovina, J.J., 2017. Variation in phytoplankton composition between two North Pacific frontal zones along 158°W during winter–spring 2008–2011. Prog. Oceanogr. 150, 3–12. https://doi.org/10.1016/j.pocean.2015.06.003.

Hyrenbach, K.D., Fernández, P., Anderson, D.J., 2002. Oceanographic habitats of two sympatric North Pacific albatrosses during the breeding season. Mar. Ecol. Prog. Ser. 233, 283–301. https://doi.org/10.3354/meps233283.

Irigoien, X., Klevjer, T.A., Røstad, A., Martinez, U., Boyra, G., Acuña, J.L., Bode, A., Echevarria, F., Gonzalez-Gordillo, J.I., Hernandez-Leon, S., Agusti, S., Aksnes, D.L., Duarte, C.M., Kaartvedt, S., 2014. Large mesopelagic fishes biomass and trophic efficiency in the open ocean. Nat. Commun. 5, 3271. https://doi.org/10.1038/ncomms4271.

Jech, J.M., Michaels, W.L., 2006. A multifrequency method to classify and evaluate fisheries acoustics data. Can. J. Fish. Aquat. Sci. 63, 386. https://doi.org/10.1139/f07-009.

Josse, E., Bach, P., Dagorn, L., 1998. Simultaneous observations of tuna movements and their prey by sonic tracking and acoustic surveys. Hydrobiologia 371, 61–69. https://doi.org/10.1023/a:1017065709190.

Juranek, L.W., Quay, P.D., Feely, R.A., Lockwood, D., Karl, D.M., Church, M.J., 2012. Biological production in the NE Pacific and its influence on air-sea CO2 flux: evidence from dissolved oxygen isotopes and O 2/Ar. J. Geophys. Res. Oceans 117, 1–23. https://doi.org/10.1029/2011JC007450.

Kaartvedt, S., Staby, A., Aksnes, D.L., 2012. Efficient trawl avoidance by mesopelagic fishes causes large underestimation of their biomass. Mar. Ecol. Prog. Ser. 456, 1–6. https://doi.org/10.3354/meps09785.

Kark, S., van Rensburg, B.J., 2006. Ecotones: marginal or central areas of transition? Isr J. Ecol. Evol. 52, 29–53. https://doi.org/10.1560/IJEE.52.1.29.

Khangaonkar, T., Nugraha, A., Yun, S.K., Premathilake, L., Keister, J.E., Bos, J., 2021. Propagation of the 2014–2016 northeast pacific marine heatwave through the salish sea. Front. Mar. Sci. 8 https://doi.org/10.3389/fmars.2021.787604.

Kloser, R.J., Ryan, T.E., Young, J.W., Lewis, M.E., 2009. Acoustic observations of micronekton fish on the scale of an ocean basin: potential and challenges. ICES (Int. Counc. Explor. Sea) J. Mar. Sci. 66, 998–1006. https://doi.org/10.1093/icesjms/fsp077.

Korneliussen, R.J., Ona, E., 2003. Synthetic echograms generated from the relative frequency response. ICES (Int. Counc. Explor. Sea) J. Mar. Sci. 60, 636–640. https://doi.org/10.1016/S1054-3139(03)00035-3.

Korneliussen, R.J., Diner, N., Ona, E., Berger, L., Fernandes, P.G., 2008. Proposals for the collection of multifrequency acoustic data. ICES (Int. Counc. Explor. Sea) J. Mar. Sci. 65, 982–994. https://doi.org/10.1093/icesjms/fsn052.

Kwiatkowski, L., Aumont, O., Bopp, L., 2019. Consistent trophic amplification of marine biomass declines under climate change. Global Change Biol. 25, 218–229. https://doi.org/10.1111/gcb.14468.

Lambert, C., Mannocci, L., Lehodey, P., Ridoux, V., 2014. Predicting cetacean habitats from their energetic needs and the distribution of their prey in two contrasted tropical regions. PLoS One 9. https://doi.org/10.1371/journal.pone.0105958.

Lebourges-Dhaussy, A., Huggett, J., Ockhuis, S., Roudaut, G., Josse, E., Verheye, H., 2014. Zooplankton size and distribution within mesoscale structures in the Mozambique Channel: a comparative approach using the TAPS acoustic profiler, a multiple net sampler and ZooScan image analysis. Deep Sea Res 2 Top Stud Oceanogr 100, 136–152. https://doi.org/10.1016/j.dsr2.2013.10.022.

Lefort, S., Aumont, O., Bopp, L., Arsouze, T., Gehlen, M., Maury, O., 2015. Spatial and body-size dependent response of marine pelagic communities to projected global climate change. Global Change Biol. 21, 154–164. https://doi.org/10.1111/gcb.12679.

Lehodey, P., 2001. The pelagic ecosystem of the tropical Pacific Ocean: dynamic spatial modelling and biological consequences of ENSO. Prog. Oceanogr. 49, 439–468. https://doi.org/10.1016/S0079-6611(01)00035-0.

Lima, I.D., 2002. Biological response to frontal dynamics and mesoscale variability in oligotrophic environments: biological production and community structure. J. Geophys. Res. 107, 3111. https://doi.org/10.1029/2000JC000393.

Lotze, H.K., Tittensor, D.P., Bryndum-Buchholz, A., Eddy, T.D., Cheung, W.W.L., Galbraith, E.D., Barange, M., Barrier, N., Bianchi, D., Blanchard, J.L., Bopp, L., Büchner, M., Bulman, C.M., Carozza, D.A., Christensen, V., Coll, M., Dunne, J.P., Fulton, E.A., Jennings, S., Jones, M.C., Mackinson, S., Maury, O., Niiranen, S., Oliveros-Ramos, R., Roy, T., Fernandes, J.A., Schewe, J., Shin, Y.J., Silva, T.A.M., Steenbeek, J., Stock, C.A., Verley, P., Volkholz, J., Walker, N.D., Worm, B., 2019. Global ensemble projections reveal trophic amplification of ocean biomass declines with climate change. Proc. Natl. Acad. Sci. U. S. A. 116, 12907–12912. https://doi.org/10.1073/pnas.1900194116.

McClatchie, S., Thorne, R.E., Grimes, P., Hanchet, S., 2000. Ground truth and target identification for f isheries acoustics. Fish. Res. 47, 173–191.

Menkes, C.E., Allain, V., Rodier, M., Gallois, F., Lebourges-Dhaussy, A. nne, Hunt, B.P.V., Smeti, H., Pagano, M., Josse, E., Daroux, A., Lehodey, P., Senina, I., Kestenare, E., Lorrain, A., Nicol, S., 2015. Seasonal oceanography from physics to micronekton in the south-west pacific. Deep Sea Res 2 Top Stud Oceanogr 113, 125–144. https://doi.org/10.1016/j.dsr2.2014.10.026.

Merrett, N.R., Gordon, J.D.M., Stehmann, M., Haedrich, R.L., 1991. Deep demersal fish assemblage structure in the porcupine seabight (Eastern North Atlantic): slope sampling by three different trawls compared. J. Mar. Biol. Assoc. U. K. 71, 329–358. https://doi.org/10.1017/S0025315400051638.

Miller, M.G.R., Carlile, N., Phillips, J.S., McDuie, F., Congdon, B.C., 2018. Importance of tropical tuna for seabird foraging over a marine productivity gradient. Mar. Ecol. Prog. Ser. 586, 233–249. https://doi.org/10.3354/meps12376.

Milligan, R.J., Sutton, T.T., 2020. Dispersion overrides environmental variability as a primary driver of the horizontal assemblage structure of the mesopelagic fish family myctophidae in the northern Gulf of Mexico. Front. Mar. Sci. 7 https://doi.org/10.3389/fmars.2020.00015.

Moku, M., Tsuda, A., Kawaguchi, K., 2003. Spawning season and migration of the myctophid fish Diaphus theta in the western North Pacific. Ichthyol. Res. 50, 52–58.
Newman, M., Wittenberg, A.T., Cheng, L., Compo, G.P., Smith, C.A., 2016. The extreme 2015/16 El Niño, in the context of historical climate variability and change. Bull. Am. Meteorol. Soc. 99, S16–S20. https://doi.org/10.1175/BAMS-D-17-0116.1.
Pacific Islands Fisheries Science Center, 2009. Water Column Sonar Data Collection (SE0902L1, EK60). NOAA National Centers for Environmental Information. NOAA NODC Acces. https://doi.org/10.7289/V57S7KQ9.
Pacific Islands Fisheries Science Center, 2011. Water Column Sonar Data Collection (SE1102L2, EK60). National Centers for Environmental Information, NOAA NODC Acces. https://doi.org/10.7289/V53776PJ.
Pacific Islands Fisheries Science Center, 2015. Water Column Sonar Data Collection (SE1501, EK60). National Centers for Environmental Information. NOAA NODC Acces. http://doi.org/10.7289/V5W093WG.
Pakhomov, E.A., Suntsov, A.V., Seki, M.P., Brodeur, R.D., Domokos, R., Pakhomova, L. G., Owen, K.R., 2010. Macrozooplankton and micronekton off Oahu island, Hawaii: composition and gear inter-calibration. In: Report of the Advisory Panel on Micronekton Sampling Inter-calibration Experiment, MIE-1, PICES Scinetific Report.
Parrish, F.A., Howell, E.A., Antonelis, G.A., Iverson, S.J., Littnan, C.L., Parrish, J.D., Polovina, J.J., 2012. Estimating the carrying capacity of French Frigate Shoals for the endangered Hawaiian monk seal using Ecopath with Ecosim. Mar. Mamm. Sci. 28, 522–541. https://doi.org/10.1111/j.1748-7692.2011.00502.x.
Pearcy, W.G., 1991. Biology of the transition region. In: Biology, Oceanography, and Fisheries of the North Pacific Transition Zone and Subarctic Frontal Zone, vol. 105. NOAA Technical Report NMFS.
Pérez-Jorge, S., Tobeña, M., Prieto, R., Vandeperre, F., Calmettes, B., Lehodey, P., Silva, M.A., 2020. Environmental drivers of large-scale movements of baleen whales in the mid-North Atlantic Ocean. Divers. Distrib. 26, 683–698. https://doi.org/10.1111/ddi.13038.
Peterson, W.T., Morgan, C.A., Peterson, J.O., Fisher, J.L., Bruke, B.J., Fresh, K., 2014. Ocean ecosystem indicators of salmon marine survival in the northern California current. NWFSC Report 8, 1–83. https://doi.org/10.1063/1.1750729.
Peterson, W.T., Bond, N.A., Robert, M., 2016. The Blob (Part Three): going, going, gone? PICES Press 24, 46–48.
Polovina, J.J., Howell, E., Kobayashi, D.R., Seki, M.P., 2001. The transition zone chlorophyll front, a dynamic global feature defining migration and forage habitat for marine resources. Prog. Oceanogr. 49, 469–483. https://doi.org/10.1016/S0079-6611(01)00036-2.
Polovina, J.J., Howell, E.A., Abecassis, M., 2008. Ocean's least productive waters are expanding. Geophys. Res. Lett. 35, 2–6. https://doi.org/10.1029/2007GL031745.
Polovina, J.J., Howell, E.A., Kobayashi, D.R., Seki, M.P., 2017. The transition zone chlorophyll front updated: advances from a decade of research. Prog. Oceanogr. 150, 79–85. https://doi.org/10.1016/j.pocean.2015.01.006.
Proud, R., Cox, M.J., Wotherspoon, S., Brierley, A.S., 2015. A method for identifying Sound Scattering Layers and extracting key characteristics. Methods Ecol. Evol. 6, 1190–1198. https://doi.org/10.1111/2041-210X.12396.
Proud, R., Cox, M.J., Brierley, A.S., 2017. Biogeography of the global ocean's mesopelagic zone. Curr. Biol. 27, 113–119. https://doi.org/10.1016/j.cub.2016.11.003.
Qiu, B., Chen, S., 2011. Effect of decadal Kuroshio Extension jet and eddy variability on the modification of North Pacific intermediate water. J. Phys. Oceanogr. 41, 503–515. https://doi.org/10.1175/2010JPO4575.1.
Receveur, A., Menkes, C., Allain, V., Lebourges-Dhaussy, A., Nerini, D., Mangeas, M., Ménard, F., 2020a. Seasonal and spatial variability in the vertical distribution of pelagic forage fauna in the Southwest Pacific. Deep Sea Res 2 Top Stud Oceanogr 175. https://doi.org/10.1016/j.dsr2.2019.104655.
Receveur, A., Vourey, E., Lebourges-Dhaussy, A., Menkes, C., Ménard, F., Allain, V., 2020b. Biogeography of micronekton assemblages in the natural park of the Coral Sea. Front. Mar. Sci. 7 https://doi.org/10.3389/fmars.2020.00449.
Receveur, A., Dutheil, C., Gorgues, T., Menkes, C., Lengaigne, M., Nicol, S., Lehodey, P., Allain, V., Menard, F., Lebourges-Dhaussy, A., 2021. Exploring the future of the coral sea micronekton. Prog. Oceanogr. 195 https://doi.org/10.1016/j.pocean.2021.102593.
Robinson, P.W., Costa, D.P., Crocker, D.E., Gallo-Reynoso, J.P., Champagne, C.D., Fowler, M.A., Goetsch, C., Goetz, K.T., Hassrick, J.L., Hückstädt, L.A., Kuhn, C.E., Maresh, J.L., Maxwell, S.M., McDonald, B.I., Peterson, S.H., Simmons, S.E., Teutschel, N.M., Villegas-Amtmann, S., Yoda, K., 2012. Foraging behavior and success of a mesopelagic predator in the northeast Pacific Ocean: insights from a data-rich species, the northern elephant seal. PLoS One 7, 1–12. https://doi.org/10.1371/journal.pone.0036728.
Roden, G.I., 1991. Subarctic-subtropical transition zone of the North pacific: large-scale aspects and mesoscale structure. In: Biology, Oceanography, and Fisheries of the North Pacific Transition Zone and Subarctic Frontal Zone, vol. 105. NOAA Technical Report NMFS.
Seki, M.P., Polovina, J.J., Kobayashi, D.R., Bidigare, R.R., Mitchum, G.T., 2002. An oceanographic characterization of swordfish (Xiphias gladius) longline fishing grounds in the springtime subtropical North Pacific. Fish. Oceanogr. 11, 251–266. https://doi.org/10.1046/j.1365-2419.2002.00207.x.
Seki, M.P., Flint, E.N., Howell, E., Ichii, T., Polovina, J.J., Yatsu, A., 2004. Transition zone. In: Perry, R.I., McKinnell, S.M. (Eds.), PICES Special Pulication No. 1 Marine Ecosystems of the North Pacific, p. 280.
Shcherbina, A.Y., Gregg, M.C., Alford, M.H., Harcourt, R.R., 2009. Characterizing thermohaline intrusions in the North Pacific subtropical frontal zone. J. Phys. Oceanogr. 39, 2735–2756. https://doi.org/10.1175/2009JPO4190.1.
Shcherbina, A.Y., Gregg, M.C., Alford, M.H., Harcourt, R.R., 2010. Three-dimensional structure and temporal evolution of submesoscale thermohaline intrusions in the north pacific subtropical frontal zone. J. Phys. Oceanogr. 40, 1669–1689. https://doi.org/10.1175/2010JPO4373.1.
Sheridan, J.A., Bickford, D., 2011. Shrinking body size as an ecological response to climate change. Nat. Clim. Change 1, 401–406. https://doi.org/10.1038/nclimate1259.
Simmonds, J.E., MacLennan, D.N., 2005. Fisheries Acoustics, second ed. Blackwell Science, Oxford.
Solberg, I., Kaartvedt, S., 2017. The diel vertical migration patterns and individual swimming behavior of overwintering sprat Sprattus sprattus. Prog. Oceanogr. 151, 49–61. https://doi.org/10.1016/j.pocean.2016.11.003.
Song, Y., Yang, J., Wang, C., Sun, D., 2022. Spatial patterns and environmental associations of deep scattering layers in the northwestern subtropical Pacific Ocean. Acta Oceanol. Sin. 41, 139–152. https://doi.org/10.1007/s13131-021-1973-1.
Suntsov, A.v., Domokos, R., 2013. Vertically migrating micronekton and macrozooplankton communities around Guam and the Northern Mariana Islands. Deep Sea Res 1 Oceanogr Res Pap 71, 113–129. https://doi.org/10.1016/j.dsr.2012.10.009.
Suntsov, A.V., Pakhomov, E.A., Michael P, Seki, Brodeur, R.D., Domokos, R., Pakhomova, L.G., 2010. Ichthyoplankton in the vicinity of Oahu islan, Hawaii. In: Report of the Advisory Panel on Micronekton Sampling Inter-calibration Experiment. MIE-1.
Sutton, T.T., 2013. Vertical ecology of the pelagic ocean: classical patterns and new perspectives. J. Fish. Biol. 83, 1508–1527. https://doi.org/10.1111/jfb.12263.
Whitney, F.A., 2015. Anomalous winter winds decrease 2014 transition zone productivity in the NE Pacific. Geophys. Res. Lett. 42, 428–431. https://doi.org/10.1002/2014GL062634.Received.
Wilson, C., Villareal, T.A., Brzezinski, M.A., Krause, J.W., Shcherbina, A.Y., 2013. Chlorophyll bloom development and the subtropical front in the North Pacific. J. Geophys. Res. Oceans 118, 1473–1488. https://doi.org/10.1002/jgrc.20143.
Woodworth-Jefcoats, P.A., Polovina, J.J., Howell, E.A., Blanchard, J.L., 2015. Two takes on the ecosystem impacts of climate change and fishing: comparing a size-based and a species-based ecosystem model in the central North Pacific. Prog. Oceanogr. 138, 533–545. https://doi.org/10.1016/j.pocean.2015.04.004.
Woodworth-Jefcoats, P.A., Polovina, J.J., Drazen, J.C., 2017. Climate change is projected to reduce carrying capacity and redistribute species richness in North Pacific pelagic marine ecosystems. Global Change Biol. 23, 1000–1008. https://doi.org/10.1111/gcb.13471.
WPRFMC, 2017. Annual Stock Assessment and Fishery Evaluation Report for the Pacific Remote Island Area Fishery Ecosystem Plan 2016. WPRFMC Report 463.
Yvon-Durocher, G., Montoya, J.M., Trimmer, M., Woodward, G., 2011. Warming alters the size spectrum and shifts the distribution of biomass in freshwater ecosystems. Global Change Biol. 17, 1681–1694. https://doi.org/10.1111/j.1365-2486.2010.02321.x.